

# A Large Throughput High Resolution Fourier Transform Spectrometer for Submillimeter Applications

M. Bin<sup>1</sup>, D.J. Benford, M.C. Gaidis<sup>2</sup>,  
T.H. Büttgenbach<sup>3</sup>, J. Zmuidzinas,  
E. Serabyn<sup>4</sup> and T.G. Phillips

Downs Laboratory of Physics  
Mail Code 320-47  
California Institute of Technology, Pasadena, CA 91125.

## Abstract

We have designed and constructed a Fourier Transform Spectrometer (FTS) for the study of submillimeter-wave mixers and optical components. The FTS has a large aperture (up to 25.4 cm) and small focal ratio (as fast as  $f/2.5$ ) to achieve a large throughput. It operates in the 100-3750 GHz ( $3.3$ - $125$   $\text{cm}^{-1}$ ) frequency range with a resolution of up to 75 MHz ( $0.0025$   $\text{cm}^{-1}$ ). Here we discuss the design goals and provide a detailed description of the construction of the FTS. In addition, we highlight the variety of studies which have been conducted with this instrument, which include characterizing SIS mixers through both direct and heterodyne detection and measuring the properties of optical materials.

**keywords:** Fourier Transform, spectroscopy, quasi-optics, heterodyne, SIS, dielectrics, submillimeterwaves, material properties

---

<sup>1</sup>Presently at TeraDyne, 30801 Agoura Rd., Agoura Hills, CA 91301

<sup>2</sup>Presently at JPL, Mail Stop 168-314, Pasadena, CA 91109

<sup>3</sup>Presently at Bach Corporation, 625 Fair Oaks Blvd., Suite 230, South Pasadena, CA 91030

<sup>4</sup>Presently at JPL, Mail Stop 171-113, Pasadena, CA 91109

## 1. Introduction

Recent advances in the technology of receivers and detectors for submillimeter astronomy have generated a need for high resolution, high sensitivity characterization of receivers and optical components. For instance, advances in the design of planar antennas and quasi-optics<sup>[1, 2, 3]</sup>, particularly in applications involving astronomy with low-noise receivers, require detailed knowledge and control of the frequency response of the mixer and associated quasi-optics. To test low-noise SIS receivers, a means of rapidly testing the frequency response of various receiver designs was needed. Fourier transform spectroscopy has been shown to be a very powerful tool in the performance analysis of SIS mixers<sup>[4, 5, 6, 7, 8, 9]</sup>. Additionally, optical components such as filters, lenses, and window materials can be studied. A precise knowledge of the refractive index and absorption coefficient of such elements is important as receivers become more nearly quantum-limited: at 492GHz, Kooi et. al.<sup>[10]</sup> measured a receiver total noise temperature of 74K, of which 52K stems from optical losses. In order to satisfy this variety of needs, we have constructed an FTS which is optimized for these kinds of studies.

A Fourier transform spectrometer is essentially a Michelson interferometer. It operates by separating the radiation from a source into two beams and then coherently recombining them to produce the output beam. Interference effects are produced by varying the relative length of optical paths traveled by the separate beams. When used without any samples in the beam paths, the signal output of the (power) detector  $I$  at a given path difference  $\delta$  is:

$$I(\delta) \propto \int_0^{\infty} S(\sigma)[1 + \cos(2\pi\sigma\delta)]d\sigma \quad (1)$$

where  $S$  is the detector response at wavenumber  $\sigma$  ( $1/\lambda$ ). The Fourier transform of this function gives the system efficiency as a function of frequency:

$$S(\sigma) \propto \int_{-\infty}^{\infty} [I(\delta) - \frac{1}{2}I(0)] \cos(2\pi\sigma\delta)d\delta. \quad (2)$$

It is thus possible to use Fourier transform spectroscopy to determine the spectral response of detectors, or, by placing an object in the combined light path and measuring response ratios, to determine the spectral transmission of optics such as windows, lenses, and filters.

To study the properties of SIS mixers at high frequencies ( $\geq 500$  GHz), an FTS with large throughput and high resolution is needed. Large

throughput in the form of large mirrors is necessary to assure a good signal to noise ratio, through collecting light from a larger solid angle or reducing spillover. A resolution much better than the IF frequency (1.5 GHz) is required to resolve the sidebands from the local oscillator in a heterodyne detection. Since commercially available Fourier Transform Spectrometers are expensive and not particularly optimized for the aforementioned features, an FTS was developed in our lab. This paper describes the FTS and gives some experimental results obtained with it, both of SIS direct and heterodyne detection and optical measurements of dielectrics.

## 2. Construction of the FTS

A block diagram of the FTS is depicted in Fig. 1. We shall discuss the design or selection criteria for each of the components in order from the source to the detector.

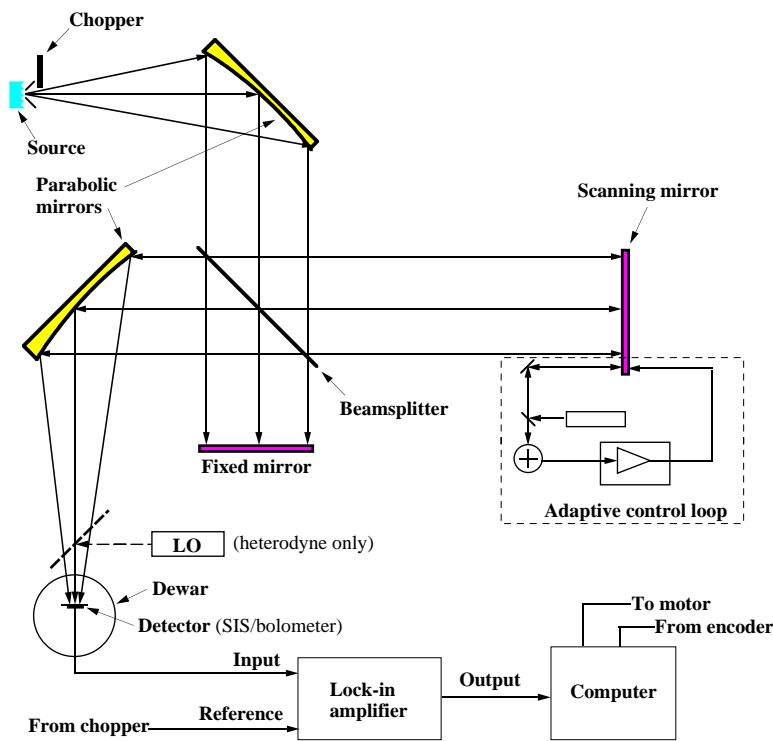


Fig. 1.— A block diagram of the FTS system.

## 2.1. The Source

The source consists of hot and cold loads, with an optical chopper blade<sup>[12]</sup> switching between the two at frequencies between  $\sim 5$  and  $\sim 250$  Hz. The hot load is a low resistance coil of NiCr alloy in a ceramic housing cavity<sup>[13]</sup>. When supplied with 6A AC (corresponding to 5 V AC), the temperature is nominally 1050°C. The temperature can be varied by changing the current. The cold load is an Eccosorb sheet<sup>[14]</sup> immersed in liquid nitrogen, serving as a 77 K blackbody. The source size is circular, about 1cm in diameter. For direct detection where the full source emitting area can reimaged onto a suitably-sized detector, an extended source causes the spectrum to spread out towards lower frequencies. This spread is  $\Delta\nu = \nu_0(\Omega/2\pi)$ ,  $\Omega$  being the solid angle subtended by the source at the collimating mirror<sup>[15]</sup>. In our FTS the source is about 64 cm away from the collimating mirror, so  $\Omega \approx \pi/(2 \times 64)^2 \approx 0.0002$ . Thus  $\Delta\nu/\nu_0 = 0.0002/2\pi \approx 3 \times 10^{-5}$ . For requirements of high resolution at high frequencies, an aperture can be used to stop down the solid angle. Alternatively, a smaller detector can be used. The effect of finite aperture size on throughput reduction becomes significant when the wavelength increases to about 1/10 of the source aperture size, or about 1mm. For our FTS this sets a rough low frequency limit at  $\nu \gtrsim c/3 \text{ mm} \sim 100 \text{ GHz}$  ( $3.3 \text{ cm}^{-1}$ ). The throughput of the FTS in the frequency region of interest is mainly determined by the beamsplitter efficiency.

## 2.2. The Mirrors and Beamsplitter

The 25.4×30.5 cm<sup>2</sup> collimating mirror is a 45° off-axis  $f/2.5$  parabola, as is the focusing mirror. It was machined from an aluminum plate with a numerically controlled mill and gold-plated afterwards, with an estimated surface accuracy of about 3  $\mu\text{m}$ . The fixed mirror and the scanning mirror are 25.4 × 25.4 cm square optical-quality first surface glass mirrors. The beamsplitter is a 35.6 cm diameter sheet of Mylar on a frame which is mounted against an annular knife-edge (rounded to prevent shearing the thin material); the knife-edge tensions the Mylar, holding it flat. Fig. 2 shows the beamsplitter efficiency calculated for 50 $\mu\text{m}$  and 100 $\mu\text{m}$  thick Mylar sheets. The 50 $\mu\text{m}$  sheet is the standard thickness, chosen for operation in the 300-1500 GHz ( $10\text{-}50 \text{ cm}^{-1}$ ) range, although various applications have used sheet thicknesses between 25 $\mu\text{m}$  and 250 $\mu\text{m}$ .

An adjustable aperture is made from a set of Eccosorb-coated aluminum sheet metal in the collimated beam between the beamsplitter and the focusing mirror. This aperture can be used to define the  $f$ -number

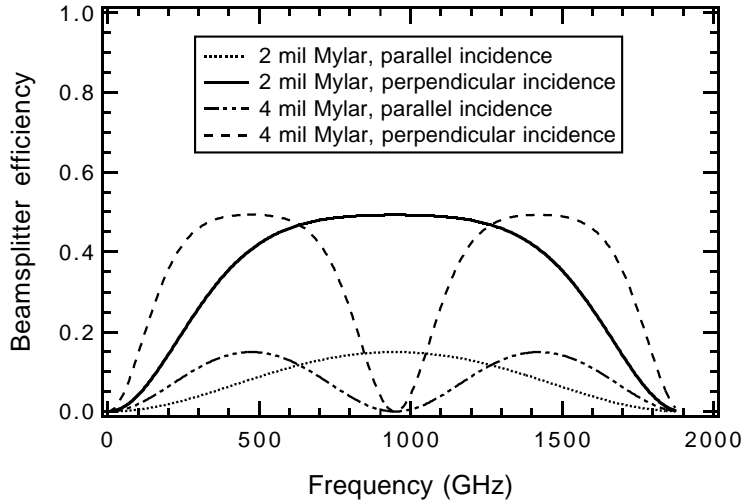


Fig. 2.— Calculated beamsplitter efficiencies for 2 mil ( $50\mu\text{m}$ ) thick and 4 mil ( $100\mu\text{m}$ ) thick Mylar sheets mounted at  $45^\circ$ . The refractive index is taken to be 1.7 for Mylar.

of the modulated beam illuminating the detector. A variety of apertures can be selected, ranging from 10 cm to  $>25$  cm, which allow for  $f$ -numbers between  $f/2.5$  and  $f/6.3$ . Smaller  $f$ -numbers match the large beams of most planar antennas used by quasi-optical SIS detectors, while larger  $f$ -numbers match the narrower beams of bolometer Winston cones.

### 2.3. The Mirror Positioner

The movable mirror is driven on a linear translation stage<sup>[16]</sup> moved by a lead screw of 2 meters length. For such long travels, although a lead screw is somewhat imprecise, a bearing slide would be extremely expensive. A step motor with a linear microstepping driver<sup>[17]</sup> moves the mirror continuously during a scan. The mirror position is read by a grating encoder and a bidirectional counter<sup>[18]</sup>. There is a TTL pulse given by the counter for every  $10\ \mu\text{m}$  of mirror motion (every  $20\ \mu\text{m}$  of optical path difference) which is used to trigger the data acquisition system so that samples are taken  $20\ \mu\text{m}$  apart in optical path difference. This sets the highest allowed frequency of the FTS to

$$\nu_{\text{max}} = \frac{c}{2 \times (20\ \mu\text{m} \times 2)} = 3750\ \text{GHz} (125\text{cm}^{-1}).$$

The position of the fixed mirror can be adjusted so that two-sided or one-sided interferograms can be taken over lengths up to the full length

of the scanning mirror travel. Only two-sided interferograms have been employed on this FTS. The advantage of taking two-sided interferograms is that one can correct for the phase error distortion in the spectrum caused by an offset of the first sample from the true zero optical path difference position<sup>[19]</sup>. A second advantage is that it helps average out the effect of any experimental asymmetries of the interferogram due to imperfect flatness or misalignment of components<sup>[20]</sup>. In order to use the FFT algorithm<sup>[21]</sup> to process the data, the number of data points should be  $2^n$ , with  $n$  an integer. For our two-sided interferograms, the longest usable scan length is limited to  $\approx 2$  meters ( $n=32$ , with the necessary extra data padded with zeros). The highest frequency resolution is therefore <sup>[15]</sup>

$$\Delta\nu = \frac{c}{2 \times \text{max. optical path difference}} = 75 \text{ MHz (0.0025cm}^{-1}\text{)}.$$

This resolution can be reduced in steps of factors of 2 from  $\Delta\nu = 114$  MHz ( $0.004 \text{ cm}^{-1}$ ) to  $\Delta\nu = 29.3$  GHz ( $\sim 1 \text{ cm}^{-1}$ ), although intermediate resolutions can also be used if a modified FFT algorithm is used.

#### 2.4. Electronic Control and Readout

The signal from the detector is sent to the input of a digital lock-in amplifier<sup>[22]</sup>, which uses a reference signal synchronized to the chopping between the hot and cold loads. The integration time constant of the lock-in is determined by the user to obtain a desirable signal to noise ratio. The speed of the scanning mirror is then set accordingly, so that the step period of the mirror is twice the integration time constant.

An Apple PowerMac 7100 serves as the computer for the FTS system control and data acquisition. A graphical user interface allows the operator to position the optics, set the parameters for an FTS scan, and perform the data analysis to measure a spectrum. The control, data acquisition and processing software is written in the LabVIEW programming environment<sup>[23]</sup> and provides real-time updating of the interferogram as it is being taken.

#### 2.5. Other FTS Hardware

The whole FTS system is built on a  $2 \times 4$  meter optical table. The optical components of the FTS system are encased in an airtight box made from 6mm thick acrylic sheets on a rigid acrylic frame. The box is purged with dry nitrogen and held at slightly over atmospheric pressure during FTS experiments to keep water absorption low. The box is sealed with

acrylic glue and silicone rubber, with vent ports to prevent overpressuring. Gasket-sealed portholes allow access to the beamsplitter, aperture, and source areas for exchanging and servicing of components. Liquid nitrogen is piped into the cold load dewar flask through a permanent stainless steel tube. Water vapor is strongly absorptive in the submillimeter, with broad absorption features at 557, 752, 988, and above 1100 GHz, as shown in figure 3. Because of the difference in absorption in the two arms of the interferometer, even small absorption losses ( $\lesssim 10\%$ ) adversely affect the quality of the data. Liquid nitrogen from a 160 liter dewar is turned into room temperature vapor through a 15 meter coiled copper pipe, immersed in temperature-controlled antifreeze. A needle valve controls the flow rate. The time to dry the box is  $\sim 6$  hours at 25% maximum flow, with an ultimate relative humidity of  $< 2\%$  as measured by a capacitive humidity meter<sup>[24]</sup>.

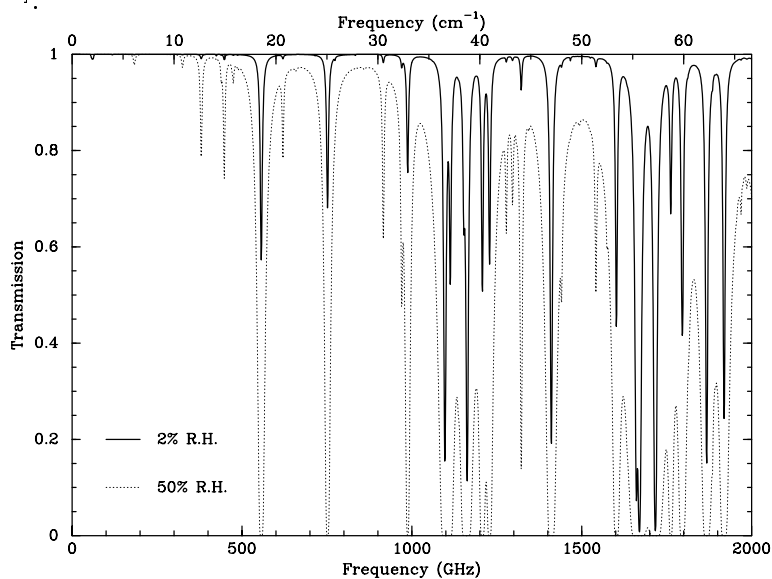


Fig. 3.— Calculated transmission of the FTS at 2% relative humidity (solid line) and 50% (dotted line), corresponding to a path length of roughly 3 meters.

## 2.6. FTS alignment

It is critical to have the movable mirror and fixed mirror each perpendicular to the incident radiation beams. Mirror tilt and lack of alignment of one mirror relative to the other can seriously affect the efficiency of the

interferometer. The requirement for alignment is that at the exit port the wave fronts of the two beams must be parallel to much better than a wavelength across the whole aperture. It can be shown that a tilt angle  $\alpha$  between the two mirrors causes reduction in the spectrum amplitude and can cause asymmetries in the interferogram<sup>[25]</sup>. The amplitude of a spectrum at wavenumber  $\sigma$  will be reduced to zero when  $\sigma\alpha l = 1/2$ , *i.e.*,  $\alpha = 0.5\lambda/l$ , where  $l$  is the linear size of the mirror, 25.4cm. The amplitude will be 95% of its original value if  $\alpha = 0.088\lambda/l$  and 50% if  $\alpha = 0.30\lambda/l$ . At higher frequencies, the alignment requirement on  $\alpha$  is more stringent.

The alignment of the scanning mirror varies as the mirror moves along the translation stage, due to the nonlinearity in the 2 meter lead screw. Over the entire scan distance the change in the normal is as large as 1.7 mrad, which corresponds to a zero amplitude response at 350 GHz. To reduce this angle an optical feedback control system was constructed.

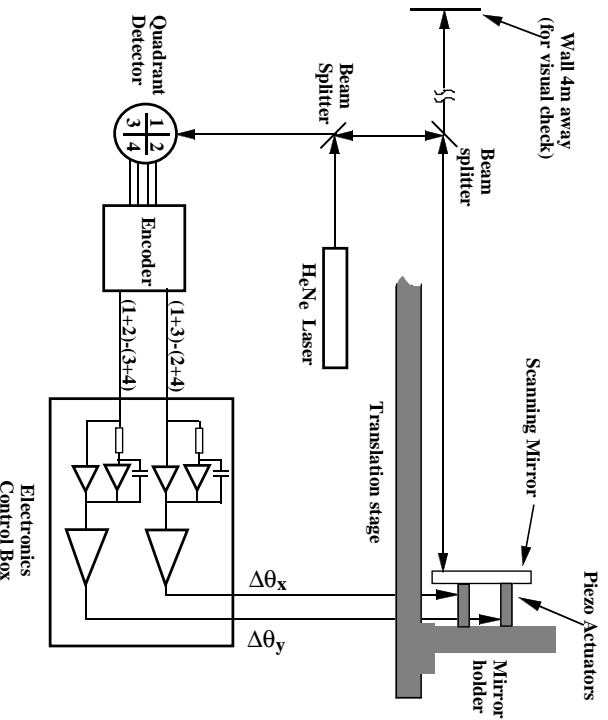


Fig. 4.—Block diagram of the optical control system for the moving mirror in the lab FTS system

Fig. 4 shows the block diagram of this feedback control system. Negative feedback is used to stabilize the normal when the mirror is moving. A two-axis tilt positioner equipped with two piezotranslators<sup>[26]</sup> holds the back of the mirror to the mirror support. By applying voltage to the two piezoelectric actuators, the mirror can be adjusted in the horizontal



and vertical directions. A He-Ne laser<sup>[27]</sup> is devoted permanently to this system. The laser is adjusted so that the incident beam to the mirror is parallel to the optical axis. The laser beam reflected back from the mirror is collected by a quadrant photon detector. The changes in the normal of the moving mirror in horizontal (x) or vertical (y) directions are then turned into error signals by an electronic decoder. These electronic error signals are amplified by a proportional-integral (PI) control circuit and sent to drive the corresponding piezoelectric actuators. Since the actuator has a large capacitance (1.6  $\mu\text{F}$ ), care must be taken to avoid turning the feedback loop into a positive one (which would be subject to oscillation) when the loop gain is larger than unity. When properly adjusted, the angular misalignment of the scanning mirror is  $< 17\mu\text{rad}$ , allowing operation with  $> 95\%$  amplitude up to 6 THz ( $200\text{ cm}^{-1}$ ).

The specifications of the FTS are summarized in Table 1.

Aperture and $f$ -number	25.4 cm maximum diameter, $f/2.5 \rightarrow f/6.3$
Frequency range	100 to 3750 GHz ( $3.3$ to $125\text{ cm}^{-1}$ )
Frequency resolution	75 MHz to 29.3 GHz ( $0.0025$ to $1\text{ cm}^{-1}$ ) (for two-sided interferogram)
Beamsplitter	tensioned sheet of $50\mu\text{m}$ Mylar (also 25, 100, $250\mu\text{m}$ available)
Source	a hot coil of NiCr alloy vs. cold Eccosorb $300\text{K} \leq T_{\text{hot}} \leq 1300\text{K}$ , $77\text{K} \leq T_{\text{cold}} \leq 300\text{K}$ , modulated optically at 5-250 Hz.
Mirror drive	2 m translation stage with DC stepper motor
Position reading	$1\mu\text{m}$ resolution grating encoder and a counter
Computer and programming	Power PC and LabVIEW
Atmosphere	Dry nitrogen, $< 2\%$ R.H. at $23^\circ\text{C}$
Mirror alignment	closed loop, accuracy $< 17\mu\text{rad}$

Table 1: Specifications of the FTS

### 3. Applications

The FTS has been used routinely for the calibration of SIS receivers in our laboratory<sup>[8, 9, 28]</sup>. It has also been used to measure the transmission and refractive index of a variety of useful submillimeter optical materials.

### 3.1. Direct detection

Using SIS junctions as direct detectors on an FTS can yield information on the SIS mixer's frequency response and thus on the performance of the tuning circuits<sup>[4, 5, 6, 7, 8, 9]</sup>. This is an effective way to check on tuning circuit design and a quick way to screen mixers.

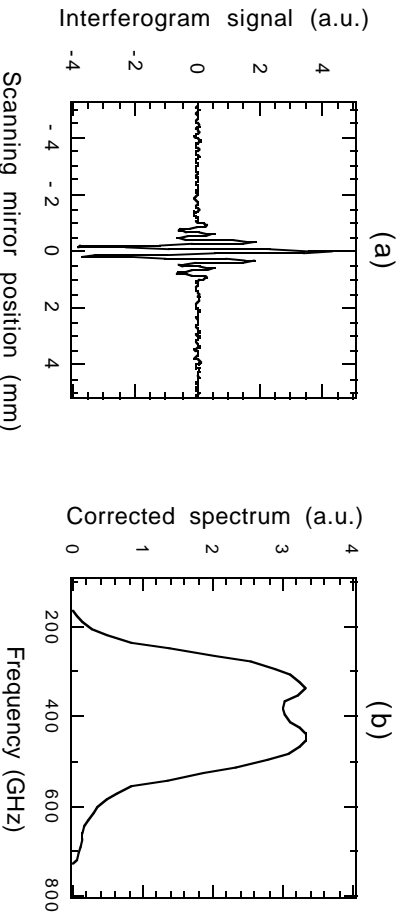


Fig. 5.— A typical interferogram (a) and the real part of its spectrum (b). The spectrum has been corrected for beamsplitter efficiency and SIS responsivity. The resolution is 14 GHz ( $0.5 \text{ cm}^{-1}$ ). The data is for a Nb SIS device with an AI tuning circuit designed to work at in the 450 GHz band.

A typical interferogram using an SIS junction as a direct detector is shown in Fig. 5, along with its spectrum corrected for beamsplitter and detector responsivity. Since no absolute calibration is available for the FTS, the absolute value of the RF coupling efficiency cannot be determined. However the FTS spectrum is still very useful in evaluating the tuning circuit design and the SIS mixer's performance by giving the shape and bandwidth of the frequency response. The frequency dependence of the direct detection and heterodyne responses correlate very well<sup>[29]</sup>. These fast and simple direct detection response measurements can thus be relied upon to predict the performance of our devices as heterodyne receivers. The spectrum shown in Fig. 5 required approximately 15 minutes to acquire with the FTS.

Fig. 6 gives another example of the SIS frequency response measured on the FTS. The device under test is a Nb-based SIS junction with an AI tuning circuit designed to work at 1050 GHz. A theoretical simulation of the device response (neglecting water absorption) is shown to compare

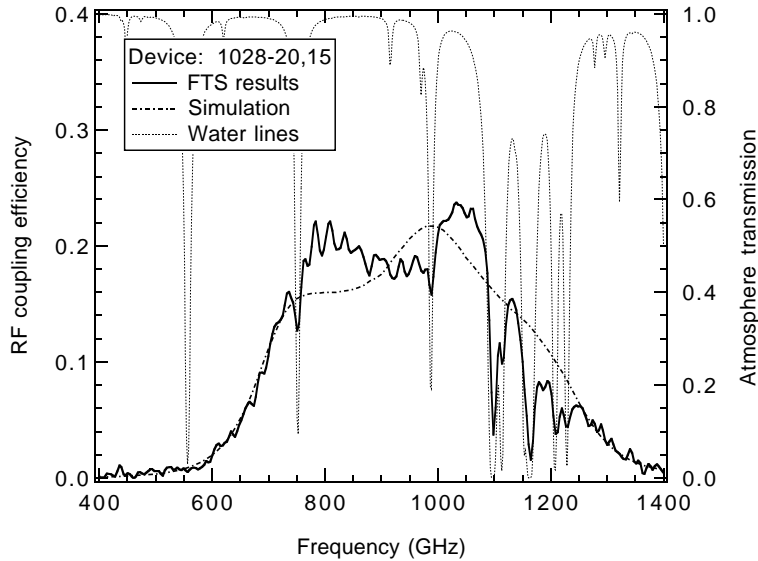


Fig. 6.— The spectrum of a Nb SIS device with Al tuning circuit designed to work at 1050 GHz. The frequency resolution for this spectrum is 3 GHz ( $0.1 \text{ cm}^{-1}$ ).

with the measurement<sup>[30]</sup>. The line absorptions due to residual water in the FTS system become severe at the high frequency end.

### 3.2. Heterodyne detection with an FTS

Early SIS receivers had narrow instantaneous bandwidths due to the lack of on-chip tuning circuits, thus it was important to know if the response of each of two sidebands was the same for a given setting of the waveguide backshorts. Even with modern broadband SIS mixers which do not need adjustable backshorts, it is still of interest to see that the responses of the two sidebands fit theory, as the frequency separation of the sidebands is increasing due to the demand for larger IF bandwidths. Heterodyne tests with the FTS provide such a measurement.

The setup for a heterodyne test on the FTS is identical to the direct-detection case except that a local oscillator is introduced by a beamsplitter in front of the dewar window, and the signal is taken at the IF power output. The incoming radiation from the FTS is same as in direct detection mode, using a chopped hot-cold load.

A heterodyne FTS interferogram and its spectrum are shown in Fig. 7. The device is an all-Nb SIS mixer which was designed to work in the

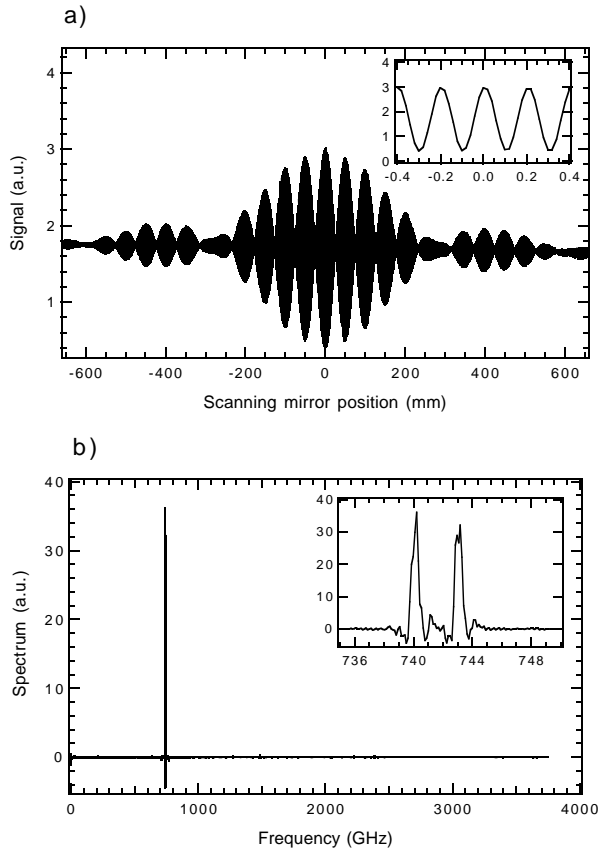


Fig. 7.— Heterodyne FTS interferogram (a) and spectrum (b) showing two sidebands. The device is an all-Nb SIS mixer optimized for the 750 GHz band.

750 GHz band<sup>[9]</sup>. Since the IF amplifier is centered at 1.5 GHz with a bandwidth of 500 MHz, a resolution of 114 MHz was used in order to separate the two sidebands. The LO frequency for this test is 742 GHz. The FTS interferogram (Fig. 7a) shows the high frequency oscillations characteristic of the 742 GHz LO (see inset), modulated by the 3 GHz sideband separation and 500 MHz IF bandwidth. The spectrum (Fig. 7b) clearly shows significant response only near the LO frequency. The IF bandwidth and double-sideband operation are evident from the inset. The negative sidelobes are due to the finite interferogram and the chosen apodization procedure in performing the inverse Fourier transform. The upper sideband peak is weaker than the lower sideband peak because of the absorption from the broad wing of the 752 GHz water line; in 10% humidity the ratio of atmospheric transmission is almost a factor of two.

### 3.3. Material Measurements

A bolometric detector is also available for use with the FTS. The instrument uses a commercially available 1.4K bolometer, Winston cone and cold amplifier<sup>[31]</sup>. In order that the light from the FTS goes through the samples in a collimated beam, an off-axis paraboloidal mirror is used to reimage the FTS output light at  $f/4.0$  into the dewar where an image of the aperture stop is placed  $\sim 2$  cm in front of the Winston cone aperture. At this point, there is a rotatable filter wheel containing 5 samples and one open port, all cooled to 1.4K. The Winston cone aperture is large enough to accept the collimated beam directly. The amplified output of the bolometer is lock-in detected, and two scans are taken, one with a sample in the beam and one without. The two are ratioed to find the absolute transmission of the material which, combined with the thickness of the material (for the simple case of a slab), allows the determination of the refractive index and absorption loss. These parameters have been measured for a variety of optical components, such as lenses, filters, and IR blocks<sup>[32]</sup>.

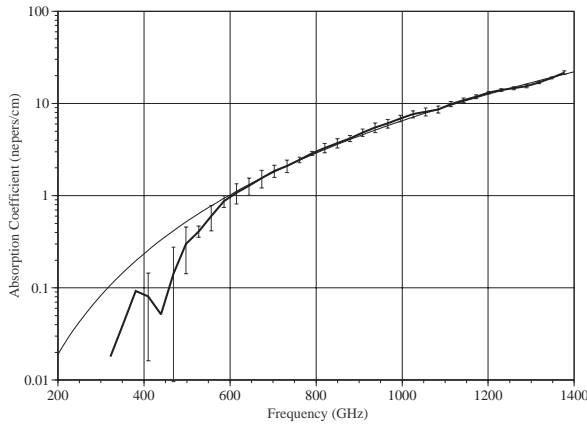


Fig. 8.— Measured absorption coefficient of Fluorogold sheet at 2K (heavy line) with a power law fit, valid above  $\sim 500$  GHz ( $\sim 15$   $\text{cm}^{-1}$ ). (thin line)

Fluorogold, a glass-fiber-filled Teflon, is a commonly used IR block as its absorption coefficient has a steep dependence on frequency when cooled. The measurements of Halpern et. al.<sup>[33]</sup> of Fluorogold rod yield an absorption coefficient at 5K of  $\alpha = 3.2 \times 10^{-5} \sigma^{3.6} \text{cm}^{-1}$  in the range  $2 < \sigma < 30 \text{cm}^{-1}$ . Our own measurement of Fluorogold sheets of  $\sim 1 - 2$  mm thickness at 2K yields  $(2.0 \pm 0.1) \times 10^{-5} \sigma^{3.63 \pm 0.02} \text{cm}^{-1}$  in the range

$15 < \sigma < 45\text{cm}^{-1}$  as shown in Fig. 8. Our lower absorption coefficient is likely due to a lower glass concentration in thin sheets as opposed to rod, as suggested by Halpern et. al.

### 3.4. Novel Filters

A harmonic filter, tuned to harmonics of the 115 GHz ( $3.8\text{ cm}^{-1}$ ) rotational transition of CO<sup>[34]</sup>, has been constructed using a matched pair of silicon disks acting as a double Fabry-Perot étalon. The transmission of this filter was measured using the FTS and is shown in Fig. 9. The measured transmission (solid line) agrees remarkably well with the theoretical transmission (dotted line). The rest frequencies of the rotational transitions are shown at the top, indicating that the filter passes the desired frequencies while strongly rejecting the out-of-band frequencies. When used with a bolometric detector on an FTS at a submillimeter telescope, the background noise power will then be reduced by a factor of  $\sim 2$ , reducing the necessary integration time by a factor of 4. This filter has been used to measure simultaneously 4 CO transitions in absorption in the atmosphere of Venus.

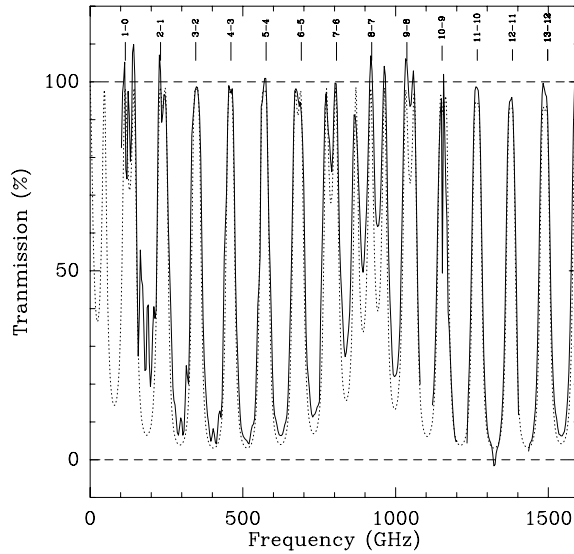


Fig. 9.— Transmission of a 115 GHz harmonic filter. The solid line is the FTS measurement, compared to the theoretical transmission (dotted line). The rest frequencies of the rotational transitions of CO are shown at the top.

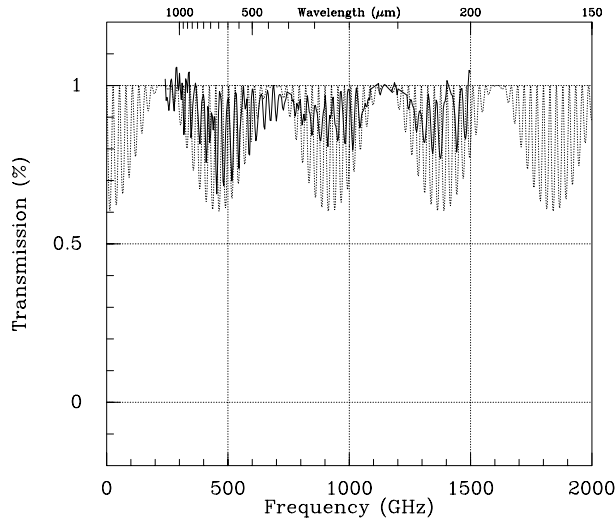


Fig. 10.— Transmission measurements (solid) and theory (dotted) for an antireflection coated quartz window designed for the 230 GHz region.

### 3.5. Optical Measurements

Quartz is a useful material both for vacuum windows and for infrared-blocking filters, because of its high transparency in the submillimeter and its relatively poor transmission in the infrared. However, its refractive index is high enough ( $n \sim 2.1$ ) to cause substantial ( $\sim 20\%$ ) reflection losses; for this reason, it is worthwhile to antireflection coat the quartz substrate with a layer of a material with index  $n \sim 1.4$  such as Teflon. We have measured the transmission of numerous windows and infrared blocks with Teflon antireflection coatings of various manufacturers (e.g. Francis Lord Optics<sup>[35]</sup>). Figure 10 is one such measurement: a 230 GHz antireflection coated window (heavy curve) compared with the theoretical design curve (light). The difference between the two most likely results from the generally poor uniformity of the thickness of the Teflon coatings, each roughly 0.2mm (0.008”) thick but visibly quite rough. Even so, the average loss around 230 GHz is decreased from roughly 20% to roughly 4%, a substantial improvement.

## 4. Acknowledgments

We wish to thank Walt Schaal and Dave Vail for helping build the FTS; Dave Woody for helpful discussions; Jacob Kooi for providing the impetus to test devices and materials; and Gabe Powers for assistance with the N<sub>2</sub> purge system.

## REFERENCES

- [1] D. B. Rutledge and M. S. Muha, "Imaging Antenna Arrays", *IEEE Trans. Antennas and Propagation*, vol. 30, pp. 535-540, 1982
- [2] G. M. Rebeiz, "Millimeter-Wave and Terahertz Integrated Circuit Antennas", *Proc. IEEE*, vol. 80, pp. 1748-1770, 1992
- [3] J. Zmuidzinas and H. G. LeDuc, "Quasi-Optical Slot Antenna SIS Mixers," *IEEE Trans. Microwave Theory Tech.*, vol. 40, pp. 1797-1804, 1992
- [4] Q. Hu, C. A. Mears, and P. L. Richards, "Measurements of integrated tuning elements for SIS mixers with a Fourier transform spectrometer," *Int. J. IR and MM Waves*, vol. 9, no. 4, pp. 303-320, 1988
- [5] T. H. Büttgenbach, R. E. Miller, M. J. Wengler, D. M. Watson, and T. G. Phillips, "A broadband low-noise SIS receiver for submillimeter astronomy," *IEEE Trans. Microwave Theory Tech.*, vol. 36, no. 12, pp. 1720-1726, 1988
- [6] G. de Lange, J. J. Kuipers, T. M. Klapwijk, R. A. Panhuyzen, H. van de Stadt, and M. W. M. de Graauw, "Superconducting resonator circuits at frequencies above the gap frequency," *J. Appl. Phys.*, vol. 77, no. 4, pp. 1795-1804, 1995
- [7] V. Y. Belitsky, S. W. Jacobsson, L. V. Filippenko, C. Holmstedt, V. P. Koshelets, and E. L. Kollberg, "Fourier transform spectrometer studies (300 -1000 GHz) of Nb-based quasi-optical SIS detectors," *IEEE Trans. Appl. Superconductivity*, vol. 5, no. 3, pp. 3445-3451, 1995
- [8] M. Bin, M. C. Gaidis, J. Zmuidzinas, T. G. Phillips, and H. G. LeDuc, "Low-noise 1 terahertz niobium superconducting tunnel junction mixer with a normal metal tuning circuit," *Appl. Phys. Lett.*, vol. 68, no. 12, pp. 1714-1716, 1996
- [9] M. C. Gaidis, H. G. LeDuc, M. Bin, D. Miller, J. A. Stern, and J. Zmuidzinas, "Characterization of low-noise quasi-optical SIS mixers for the submillimeter band," *IEEE Trans. Microwave Theory Tech.*, vol. 44, no. 7, pp. 1130-1139, 1996
- [10] J.W. Kooi, M. Chan, B. Bumble, H.G. LeDuc, P. Schaffer, and T.G. Phillips, "230 and 492 GHz low-noise SIS wave-guide receivers employing tuned NB/AlOx/Nb tunnel-junctions", *Int. J. IR and MM Waves* vol. 16, pp. 2049-2068, 1995
- [11] E. Serabyn, T. G. Phillips, and C. R. Masson, "Surface figure measurements of radio telescopes with a shearing interferometer," *Appl. Optics*, vol. 30, no. 10, pp. 1227-1241, 1991
- [12] SR-540 Optical Chopper, Stanford Research Systems, 1290-D Reamwood Ave., Sunnyvale, CA 94089
- [13] Filament #17-1079, Perkin Elmer Corp., 7421 Oranewood Ave.,



- Garden Grove, CA 92641.
- [14] Eccosorb AN-72, Emerson & Cuming, 869 Washington St., Canton, MA 02021.
  - [15] R. J. Bell, *Introductory Fourier transform spectroscopy*, Academic Press: New York and London, 1972
  - [16] Electric Cylinder model RS-2205 A-MS5-HC-Q2, Industrial Devices Corporation, 64 Digital Drive, Novato, CA 94949; (800) 747-0064
  - [17] Compumotor Low-Noise linear microstepping amplifier (LN Drive), Compumotor Division of Parker Hannifin, 5500 Business Park Drive, Rohnert Park, CA 94928
  - [18] Linear Encoder LS-603, Bidirectional Counter VRZ-405, Heidenhain Corporation, 115 Commerce Drive, Schaumburg, IL 60173
  - [19] H.W. Schnopper & R.I. Thompson, "Fourier Spectrometers," in *Methods of Experimental Physics 12A: Astrophysics*, ed. by N. Carleton, Academic Press Inc., New York, 1974
  - [20] P. L. Richards, "Fourier transform spectroscopy," in *Spectroscopic Techniques for Far-infrared, Submillimeter, and Millimeter Waves*, ed. by D. H. Martin, North-Holland Pub. Co., New York Wiley: Amsterdam, 1967
  - [21] O. E. Brigham, *The fast Fourier transform*, Englewood Cliffs, N. J., Prentice-Hall, 1974
  - [22] SR-830 Lock In Amplifier, Stanford Research Systems, 1290-D Reamwood Ave., Sunnyvale, CA 94089
  - [23] LabVIEW, National Instruments, 6504 Bridge Point Parkway, Austin, TX 78730-5039 (512) 794-0100
  - [24] P-37951-00 Thermohygrometer, Cole-Parmer Instrument Co., 625 E. Bunker Ct., Vernon Hills, IL 60061
  - [25] Charles S. Williams, "Mirror misalignment in Fourier spectroscopy using a Michelson interferometer with circular aperture," *Appl. Optics*, vol. 5, no. 6, pp. 1084-85, 1966
  - [26] Piezoelectric Tilt Positioner P-840, Physik Instrumente, Main U.S. office, 3001 Redhill Ave. Bldg. 5-102, Costa Mesa, CA 92626
  - [27] Model 1104P, Uniphase Lasers, 163 Baypointe Parkway, San Jose, CA 95134
  - [28] J. W. Kooi, M. S. Chan, M. Bin, B. Bumble, and H. G. LeDuc, "The development of an 850 GHz waveguide receiver using tuned SIS junctions on  $1\mu\text{m}$   $\text{Si}_3\text{N}_4$  membranes," *Int. J. IR and MM Waves*, vol. 16, pp. 349-362, 1995
  - [29] M. Bin, M. C. Gaidis, J. Zmuidzinas, T.G. Phillips & H.G. LeDuc, "Quasi-optical SIS mixers with normal metal tuning structures," *IEEE Trans. Appl. Superconductivity*, vol. 7, pp3584-3588, 1997
  - [30] M. Bin, M. C. Gaidis, D. Miller, J. Zmuidzinas, T. G. Phillips, and H.

- G. LeDuc, "Design and characterization of a quasi-optical SIS receiver for the 1 THz band," Proc. Seventh Intl. Symp. Space Terahertz Tech., March 12-14, 1996 Charlottesville, VA 22903
- [31] Infrared Labs, 1808 East 17th Street, Tucson, AZ 85719-6505; (520) 622-7074
- [32] D. J. Benford, J. W. Kooi, and E. Serabyn, "Spectroscopic measurements of optical components around 1 Terahertz", Proc. Ninth Intl. Symp. Space Terahertz Tech., March 1998, JPL, Pasadena, CA
- [33] M. Halpern, H. P. Gush, E. Wishnow, and V. De Cosmo, *Applied Optics*, vol. 25, no. 6, pp. 565-570, 1986
- [34] D. J. Benford, S. Wu, J. Pardo and E. Serabyn, 1999, *Applied Optics*, in preparation
- [35] Francis Lord Optics, 33 Higginbotham Rd., Gladesville NSW 2111, Australia; 001-61-9807-1444